Extreme Mechanics Letters 40 (2020) 100879

Contents lists available at ScienceDirect

Extreme Mechanics Letters

journal homepage: www.elsevier.com/locate/eml

Instabilities of embedded cylindrical inclusions undergoing isotropic swelling or growth

John W. Hutchinson

School of Engineering and Applied Sciences, Harvard University, United States of America

ARTICLE INFO

Article history:
Received 18 May 2020
Accepted 7 July 2020
Available online 21 July 2020

Keywords:
Buckling of rods
Neo-Hookean materials
Growth-driven instability
Bifurcation

ABSTRACT

Infinite circular cylindrical elastic inclusions, or rods, embedded in an unbounded elastic matrix display various modes of instability when they undergo sufficiently large expansion due to either swelling or volumetric growth. In this letter two modes of instability are examined: sinusoidal axisymmetric modes and sinusoidal bending modes. The rod and the matrix are neo-Hookean materials, and the full range of the modulus ratio of rod to matrix is considered. In the primary case examined, deformation is driven by an isotropic volumetric expansion, or transformation, of the rod. A three-dimensional bifurcation analysis of the rod constrained by the matrix reveals the onset of the critical instability mode as dependent on the modulus ratio. Comparisons with related results are discussed, including the compressive buckling of a stiff rod in a compliant matrix and the other limit when the modulus of the rod is very small compared to that of the matrix and behaves effectively as a fluid exerting pressure on the wall of the matrix cavity.[1]

1. Introduction

The buckling of rods and fibers supported by compliant matrices has long been of interest in many applications particularly for fiber reinforced composites and more recently for fine filament wires embedded in compressed soft elastomeric materials (see references in [1,2]). Other recent studies have focused on shapes that develop when growing fibrils and tendrils are constrained by their surrounding medium [3]. In this letter results are presented for axisymmetric and bending instabilities that occur when a cylindrical rod embedded in an unbounded elastic matrix undergoes isotropic growth, equivalent to isotropic swelling. This form of growth is called volumetric growth and is one of the simplest of the many possibilities discussed in the recently published book on the mechanics of growth [4].

The present work focusses on the basic mechanics of the instability of compressed elastic rods surround by, and bonded to, an elastic matrix. The rod and matrix are each taken to be incompressible neo-Hookean materials. A bifurcation analysis is performed revealing the competition between axisymmetric instabilities and bending-like instabilities. The analysis is carried out within an exact three-dimensional, finite strain framework. The full range of rod to matrix moduli ratios is analyzed, from stiff rods in compliant matrices to very compliant rod-like inclusions in a stiff matrix. The results presented here can serve as a benchmark for more approximate analyses such as those based on one dimensional beam–spring models widely used to represent stiff rods in compliant matrices. Systems where the rod and matrix moduli are comparable are also considered and contact is made with earlier work related to each of the two moduli ratio limits.

2. The bifurcation problem

2.1. Pre-bifurcation solution

For brevity the cylindrical inclusion is referred to as the 'rod' and the surrounding unbounded elastic medium to which it is bonded will be called the 'matrix'. The swelling, or growth, of the rod is taken to be an isotropic expansion. The additional deformation will be modeled as being an incompressible neo-Hookean elastic solid with shear moduli in the rod and matrix denoted by μ_R and μ_M respectively. With (r, θ, z) denoting cylindrical coordinates of material points in the undeformed state, the radius of the undeformed rod prior to growth is taken to be r_0. The rod/matrix combination is infinite in the z-direction and extends to infinity in the radial direction. The pre-bifurcation deformation and stresses are driven by the isotropic expansive transformation in the rod material. This expansion is characterized by the stretch λ_G which would occur stress-free in the material if it were unconstrained. The constraint of the matrix generates the stresses and strains in the rod and in the matrix in the pre-bifurcation state.

In the pre-bifurcation state the principal stretches are oriented in the radial, circumferential and axial directions and are

E-mail address: hutchinson@husm.harvard.edu.

[1] Contributed to celebrate the awarding of the Prager medal to Prof. Horacio Espinosa.

https://doi.org/10.1016/j.eml.2020.100879
2352-4316/

denoted by $(\lambda_r, \lambda_\theta, \lambda_z)$. For an incompressible neo-Hookean material, the strain energy density is given in terms of the principal (stress-producing, or elastic) stretches by

$$W = \frac{1}{2}\mu\left({\lambda_r}^2 + {\lambda_\theta}^2 + {\lambda_z}^2 - 3\right) \text{ subject to } \lambda_r\lambda_\theta\lambda_z = 1 \tag{1}$$

where μ_R pertains to the rod and μ_M to the matrix. The true, Cauchy, stresses are given by

$$\sigma_r = \mu{\lambda_r}^2 - q,\ \ \sigma_\theta = \mu{\lambda_\theta}^2 - q,\ \ \sigma_z = \mu{\lambda_z}^2 - q \tag{2}$$

and q is not determined by the constitutive relation but by the equilibrium conditions.

The solution to the *pre-bifurcation problem* is a classic finite strain elasticity problem and readily obtained. The elastic stretches and stresses in the rod are uniform. The unbounded matrix constrains the rod in the axial direction such that there is no net stretch and, consequently, the axial elastic stretch in the rod is $\lambda_z = 1/\lambda_G$. Circular symmetry and the incompressibility condition on the elastic stretches give the remaining two stress-producing stretches in the rod as $\lambda_r = \lambda_\theta = {\lambda_G}^{1/2}$. The radius of the cylindrical rod in the pre-bifurcation state is $R_0 = {\lambda_G}^{3/2} r_0$. In the matrix, the pre-bifurcation solution has $\lambda_z = 1$ and $\lambda_\theta = 1/\lambda_r$. Incompressibility and circular symmetry dictate that the radial position of a material point at r in the undeformed state will be $R = \sqrt{{R_0}^2 + (r^2 - {r_0}^2)}$ in the deformed state. Thus, the distribution of stretches in the matrix can be expressed in terms of the variable locating points in the undeformed state, r, or in the pre-bifurcation state, R, as

$$\begin{aligned}\lambda_\theta &= 1/\lambda_r = R/r = \sqrt{1 + ({\lambda_G}^3 - 1){r_0}^2/r^2}\\ &= 1/\sqrt{1 - (1 - {\lambda_G}^{-3}){R_0}^2/R^2},\\ R_0 &= {\lambda_G}^{3/2} r_0\end{aligned} \tag{3}$$

The stresses in (2) are determined apart from the pressure-related term q. The equation of radial equilibrium in the pre-bifurcation state can be integrated from $R = \infty$ where $\sigma_r = 0$ to give

$$\begin{aligned}&\sigma_r(R) = -\frac{1}{2}\mu_M\left\{\ln(1+T) + \frac{T}{1+T}\right\} \text{ with}\\ &T = \frac{1 - {\lambda_G}^3}{(R/R_0)^2 - (1 - {\lambda_G}^3)}\end{aligned} \tag{4}$$

From (2), the other two stress components in the matrix are

$$\sigma_\theta = \sigma_r + \mu_M({\lambda_\theta}^2 - {\lambda_r}^2),\ \ \sigma_z = \sigma_r + \mu_M({\lambda_z}^2 - {\lambda_r}^2) \tag{5}$$

The radial stress at the rod/matrix interface is

$$\sigma_r(R_0) = -\frac{1}{2}\mu_M\left\{3\ln\lambda_G + 1 - {\lambda_G}^{-3}\right\} \tag{6}$$

The uniform stresses in the rod satisfying continuity of traction across the interface are

$$\begin{aligned}&\sigma_r = \sigma_\theta = -\frac{1}{2}\mu_M\left\{3\ln\lambda_G + 1 - {\lambda_G}^{-3}\right\},\\ &\sigma_z = -\frac{1}{2}\mu_M\left\{3\ln\lambda_G + 1 - {\lambda_G}^{-3}\right\} + \mu_R\left({\lambda_G}^{-2} - \lambda_G\right)\end{aligned} \tag{7}$$

2.2. Eigenvalue problem governing bifurcation

The problem for the critical condition governing the onset of bifurcation can be formulated in several ways. For example, one can work with variables dependent on the coordinates (r, θ, z) identifying material points in the undeformed state, or one can take the deformed state at bifurcation as reference with variables dependent on coordinates (R, θ, z). Here, the latter choice has been made. Furthermore, one can work with the quadratic bifurcation functional or one can work directly with differential equations which are generated by rendering the bifurcation functional stationary. The different choices are illustrated in the paper [5] on a basic problem involving a uniformly stressed block of a single material. The approach used here, which is given in Section 4, works directly with the partial differential equations governing the bifurcation problem. As a check on our results we have also employed a method based on the bifurcation functional.

The increments of the displacements and of q in the bifurcation mode are denoted by $(\dot{u}_r, \dot{u}_\theta, \dot{u}_z, \dot{q})$. The partial differential equations governing the bifurcation mode and the associated eigenvalue separate exactly into sinusoidal variations of the form

$$\begin{aligned}\dot{u}_r &= U(R)\cos m\theta \sin\beta z\\ \dot{u}_\theta &= V(R)\sin m\theta \sin\beta z\\ \dot{u}_z &= W(R)\cos m\theta \cos\beta z\\ \dot{q} &= Q(R)\cos m\theta \sin\beta z\end{aligned} \tag{8}$$

where $m = 0$ (with $V = 0$) generates axisymmetric modes and $m = 1$ generates bending-like modes. The axial wavelength of the mode is $L = 2\pi/\beta$. When substituted into the partial differential equations in Section 4, a set of ordinary differential equations (odes) for (U, V, W, Q) is obtained. This set can be reduced to a set of sixth first order linear odes (four first order odes for $m = 0$) with variable coefficients derived analytically from the pre-bifurcation solution. The continuity conditions at the rod/matrix interface, $R = R_0$, require continuity of the displacement increments and the traction increments. Homogeneous boundary conditions at $R = 0$ which depend on m are given in Section 4, and (U, V, W, Q) must vanish as $R \to \infty$. The eigenvalue of the system is the swelling, or growth, parameter λ_G. The sixth order system of odes (and fourth order system) is an exact reduction of the eigenvalue problem. The search for the critical eigenvalue for either $m = 0$ or $m = 1$ involves incrementing the value of λ_G and evaluating the eigenvalue criterion as discussed in Section 4. Thus, at each evaluation step, the reference geometry is the pre-bifurcation state given in Section 2.1. A numerical ode solver [6] has been used to generate the solutions. The numerical results are accurate to the values listed, which is generally 4 significant places for the critical strains and stresses and 3 significant places for the wavelengths.

3. Critical strains and stresses at the onset of instability and associated modes

Figs. 1 and 2 provide an overview of the instability modes for the entire range of the matrix/rod modulus ratio. The plot of the engineering growth strain, $\varepsilon_G = \lambda_G - 1$, at bifurcation for the axisymmetric mode ($m = 0$) and bending mode ($m = 1$) reveals that the lowest, or critical, bifurcation is the bending mode if $\mu_M/\mu_R < 5$ and the axisymmetric mode for $\mu_M/\mu_R > 5$. The bifurcation growth strains plotted in Fig. 1 have been minimized with respect to the wavelength for each of the two modes, and those critical wavelengths are plotted in Fig. 2, normalized by the radius of the rod at bifurcation, $R_0 = {\lambda_G}^{3/2} r_0$. Conversion of results to the original undeformed geometry can be made using the results in Section 2, and the stretches and stress in the rod and matrix at bifurcation are given in terms of λ_G by (3)–(7). The numerical results used to plot Figs. 1 and 2 are presented in Table 1.

If the rod and the matrix have the same shear moduli, the critical growth strain, axial stress and wavelength are

$$\left.\begin{aligned}&\varepsilon_G = 1.741\\ &\sigma_{zz}/\mu_R = 4.598\\ &L/R_0 = 0.421\end{aligned}\right\} m = 0 \text{ and}$$
$$\left.\begin{aligned}&\varepsilon_G = 1.326\\ &\sigma_{zz}/\mu_R = 3.869\\ &L/R_0 = 3.10\end{aligned}\right\} m = 1 \text{ for } \mu_M/\mu_R = 1 \tag{9}$$

Table 1
Values for the growth model.

$m=0$, μ_M/μ_R	λ_G	L/R_0	$m=1$, μ_M/μ_R	λ_G	L/R_0
1	2.741	0.421	1	2.326	3.10
1.5	2.882	0.466	2/3	2.086	3.56
2	2.982	0.506	1/2	1.925	3.95
3	3.106	0.580	1/3	1.750	4.60
5	3.207	0.702	1/5	1.562	5.55
10	3.228	0.916	0.1	1.375	7.12
20	3.160	1.19	0.05	1.248	9.00
50	3.037	1.58	0.02	1.144	12.2
100	2.965	1.86	0.01	1.095	15.2
1000	2.869	2,42	0.001	1.0251	29.7
10 000	2.857	2.53	0.0001	1.00694	55.6
			2	2.770	2.31
			10	3.338	1.09
			100	3.343	1.13

These results involve growth strains and elastic strains which are relatively deep into the finite strain range. Consequently, the numerical values determined in (9), as well as for the other results in Figs. 1 and 2 for $\mu_M/\mu_R > 0.01$, are dependent on the fact that the constitutive model is neo-Hookean model. However, one can expect similar qualitative trends for other elastomeric models.

The separation between the two eigen-strains and stresses in (9) is substantial with the bending mode being critical. It is worth noting that the logarithmic scale used in Fig. 1 tends to mask the separation between the eigen-states. This is true when μ_M/μ_R becomes large. For example, for $\mu_M/\mu_R = 50$, the critical grow strain and axial stress in the rod are both about 15% smaller for the axisymmetric mode than the bending mode.

In analyzing the growth bifurcation problem, we have checked that short wavelength sinusoidal interface wrinkles and creases (scale-independent with arbitrarily short wavelengths) oriented either parallel to the circumferential direction or the axial direction do not occur prior to the modes two modes of interest discussed above. Apart from the left end of the curve for the axisymmetric mode ($m = 0$) in Fig. 1, all the bifurcation results in Fig. 1 lie well below the onset of short wavelength interface wrinkles. The left end of the curve for $m = 0$ at $\mu_M/\mu_R \cong 0.7$ is approximately the point where this curve intersects the condition for interface wrinkles. Further discussion of the interface instability bifurcations is given in Section 4.

We next discuss, in turn, how the two limits seen in Fig. 1, a rod in a highly compliant matrix on the left and a soft cylindrical inclusion surrounded by a stiff matrix on the right, relate to existing results in the literature.

3.1. Stiff rod in a compliant matrix $\mu_M < \mu_R$

Fig. 3 compares the results obtained in this paper for the axial stress in the rod at the bending instability ($m = 1$) based on the exact 3-D formulation for neo-Hookean materials (with isotropic growth of the rod) with what, as far as we know, are the most accurate 1-D modeling results in the literature for an axially compressed rod surrounded by a compliant matrix. The plot on the left presents the critical compressive axial stress $-\sigma_z$ in the rod at bifurcation normalized by μ_R for ratios μ_M/μ_R less than 1, while the plot on the right presents the associated wavelength.

Most of the earlier modeling has represented the rod by a compressed Euler–Bernoulli beam with bending stiffness, $E_R I$ (with E_R as Young's modulus of the rod and I as the moment of area of its cross-section) whose transverse deflection is resisted by a distributed linear spring system having a stiffness K with units of force per deflection per unit length of rod. The beam theory equation governing the eigen-value problem for the critical axial stress at which the rod buckles is

$$E_R I\frac{d^4w}{d^4z} - \sigma_z A\frac{d^2w}{d^2z} + Kw = 0 \tag{10}$$

where for a cylindrical rod with radius R_0, $A = \pi {R_0}^2$ and $I = \pi {R_0}^4/4$. The authors of [7] (see also [1]) made use of the solution for a cylindrical cavity in an infinite isotropic linear elastic medium subject to sinusoidally varying tractions in the axial direction on the cavity wall to derive the following expression for the wavelength-dependent stiffness representing the restoring force exerted by the matrix

$$K(\beta R_0) = \frac{8\pi\mu_M}{2K_0(\beta R_0) + \beta R_0 K_1(\beta R_0)} \tag{11}$$

The above expression has been specialized to the incompressible case with a matrix Poisson ratio of ½. As before, $L/R_0 = 2\pi/(\beta R_0)$ with K_0 and K_1 as modified Bessel functions of the second kind of order 0 and 1. Substitution of eigen-solutions of the form $w = \sin(\beta z)$ into (10) with $E_R = 3\mu_R$ gives the associated eigen-stress

$$\frac{-\sigma_z}{\mu_R} = \frac{3}{4}(\beta R_0)^2 + \frac{K(\beta R_0)}{\pi\mu_R(\beta R_0)^2} \tag{12}$$

Elementary numerical methods minimize this eigen-stress with respect to βR_0 generating the curves in Fig. 3. Similar curves based on this model were presented in [1]. Numerical fits to the results of the present model for small values of the modulus ratio have been generated by passing a straight line in the log–log plot through the values in Table 1 at $\mu_M/\mu_R = 0.0001$ and 0.001. These give

$$\frac{-\sigma_z}{\mu_R} = 2.58\left(\frac{\mu_M}{\mu_R}\right)^{0.510} \text{ and } \frac{L}{R_0} = 4.54\left(\frac{\mu_M}{\mu_R}\right)^{-0.272} \tag{13}$$

and are plotted in Fig. 3.

Over a substantial range of the moduli ratio for μ_M/μ_R, almost as large as 0.1 in Fig. 3, the results for the axial stress at bifurcation the rod (and for the associated wavelength of the mode) are in close agreement. This is in spite of the fact that the beam–spring model ignores the pre-bifurcation stress in the matrix. To gain further insight into this class of problems, we have generated results using the present 3-D approach for another related problem—the buckling of an embedded rod where the rod and matrix system is unstressed at zero load and is compressed uniformly parallel to the cylindrical axis with $\lambda_z < 1$. For this problem the pre-bifurcation stresses are uniform in the rod and in the matrix with $\sigma_r = \sigma_\theta = 0$ throughout and

$$\sigma_z = \mu_R({\lambda_z}^2 - {\lambda_z}^{-1}), \quad \sigma_z = \mu_M({\lambda_z}^2 - {\lambda_z}^{-1})$$

in the rod and matrix respectively. The structure of the two problems is similar, with the details laid out in Sections 2 and 4 still applicable apart from the difference in the pre-bifurcation stress.

Fig. 4 presents the axial stress in the rod at bifurcation for the two 3-D problems. Except for moduli ratios μ_M/μ_R larger than 0.1, the critical stresses for the two problems are close. The differences observed in the range where the modulus ratio is not small is not surprising because the different states of pre-bifurcation stress in the rod and in the matrix become important. In this range, finite strain considerations and the specific constitutive model itself also become important. In the range where the growth strain ε_G at bifurcation is not small, one would expect differences to arise between isotropic growth considered in this paper and, for example, anisotropic growth in which the rod extends but does not expand radially.

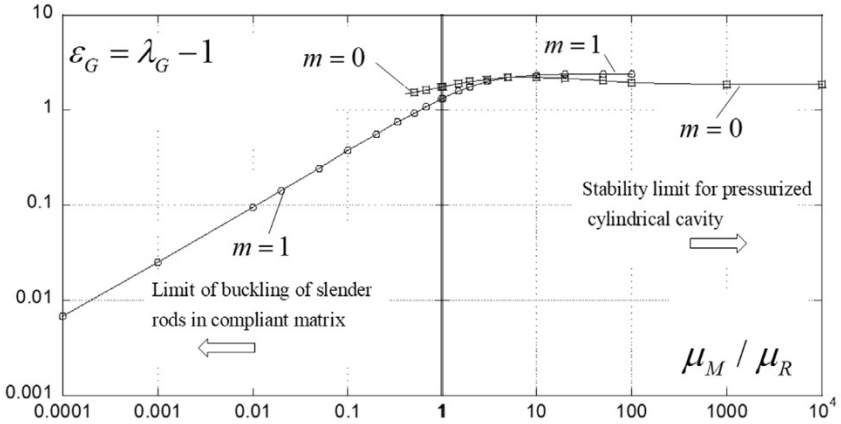

Fig. 1. Critical growth strain $\varepsilon_G = \lambda_G - 1$ at bifurcation for the axisymmetric mode ($m = 0$) and the bending mode ($m = 1$) for infinitely long cylindrical inclusions (rods) embedded with an unbounded matrix. The materials are neo-Hookean and incompressible with μ_M as the shear modulus of the matrix and μ_R as that of the rod. The associated mode axial wavelengths are given in Fig. 2.

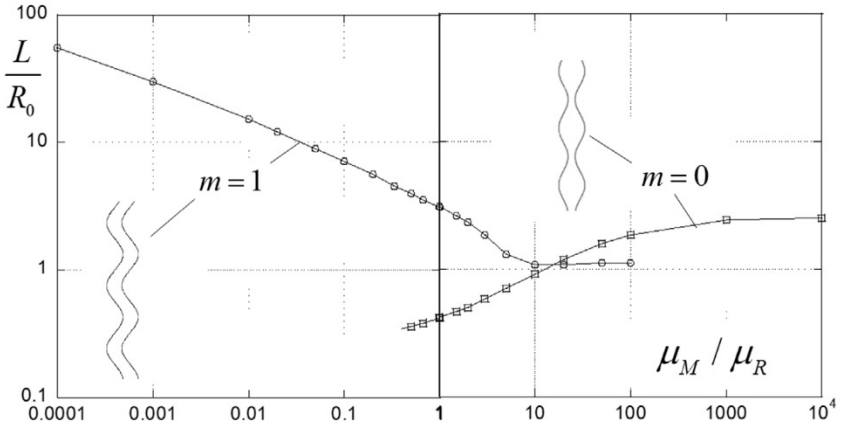

Fig. 2. Axial wavelengths associated with the critical growth strain at bifurcation for the axisymmetric mode ($m = 0$) and the bending mode ($m = 1$), plotted as L/R_0 where R_0 is the radius of the rod at the associated bifurcation strain, $R_0 = {\lambda_G}^{3/2} r_0$.

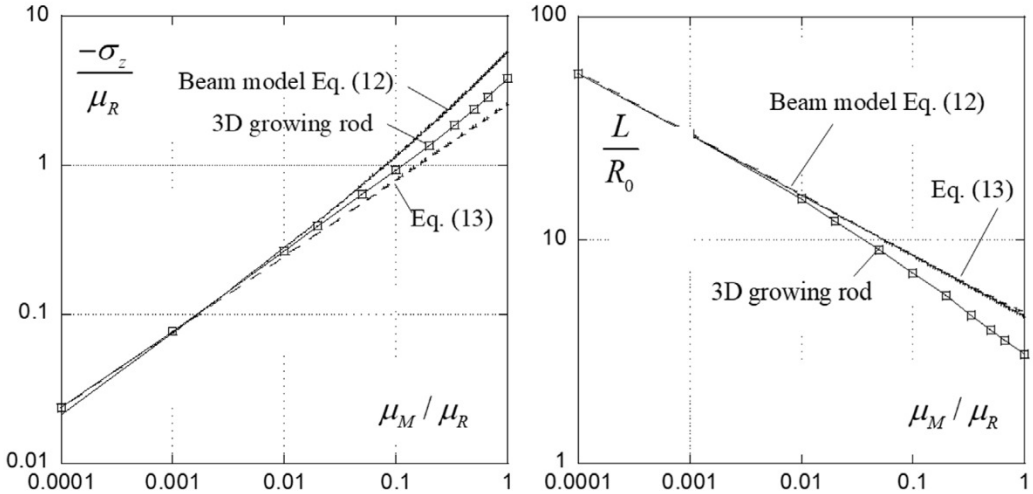

Fig. 3. Axial stress in the rod at bifurcation and axial wavelength of the associated mode for the present 3-D growth problem compared with the buckling stress of a compressed rod embedded in an elastic matrix as predicted by the beam–spring model (12). Also shown as dashed lines are the numerical fits in (13).

3.2. Soft cylindrical inclusion in a relatively stiff matrix $\mu_M > \mu_R$

The other limit when μ_M/μ_R becomes large in Figs. 1 and 2 approaches a recently published result for the instability of a cylindrical cavity containing a fluid under pressure [8]. Recall that for $\mu_M/\mu_R > 5$ the lowest bifurcation mode is axisymmetric ($m = 0$). It can be seen in Fig. 1 that for $\mu_M/\mu_R > 100$ the critical growth strain has almost attained the limit. For $\mu_M/\mu_R = 10^4$, the numerical results from Table 1 give

$$\lambda_G = 2.857, \quad \sigma_r/\mu_M = -2.054, \quad L/R_0 = 2.53 \tag{14}$$

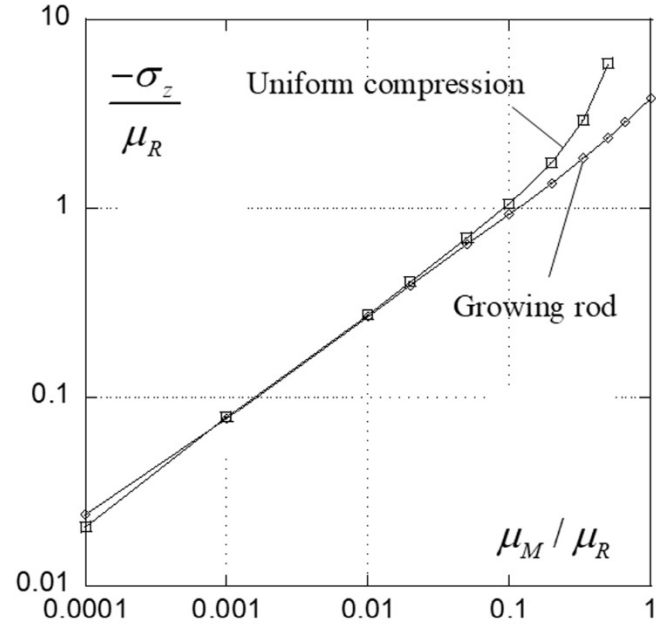

Fig. 4. Axial stress in the rod at bifurcation for two 3-D problems, uniform compression of the rod/matrix combination and the growing rod.

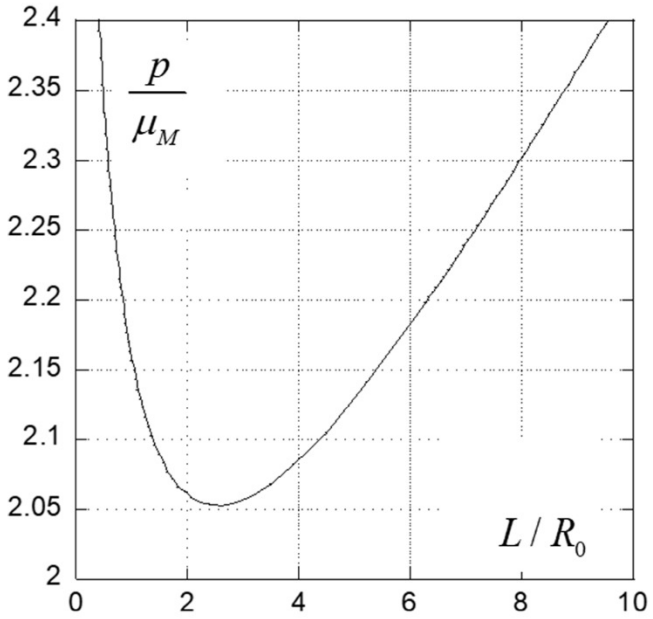

Fig. 5. Eigen-pressure spectrum for a pressurized cylindrical cavity in an unbounded neo-Hookean material.

The problem of an unbounded neo-Hookean material containing an infinitely long circular cylindrical cavity subject to fluid pressure p is in the class of problems falling into the framework laid out in Section 2. We have separately analyzed the pressurized cavity problem obtaining the following results for the critical bifurcation (with $m = 0$):

$$p/\mu_M = 2.054, \quad L/R_0 = 2.62, \quad R_0/r_0 = 4.825, \quad L/r_0 = 12.6 \quad (15)$$

The value of the wavelength differs slightly from the value given in [8] but the critical pressure is in complete agreement with their result. Moreover, this pressure is the same as that for the radial stress acting on the matrix interface for the case in (14) with $\mu_M/\mu_R = 10^4$. The shear modulus of the 'rod' is so low compared to that of the matrix that the rod functions effectively as a fluid supporting a stress state that is nearly a pure hydrostatic pressure. For completeness, we have included Fig. 5 displaying the eigen-pressure spectrum plotted in terms of the wavelength normalized by the radius of the cavity at bifurcation, R_0. Fig. 5 reveals a sharply defined minimum in the spectrum, which is less clear when the spectrum is plotted against L/r_0.

4. Formulation and reduction of the 3D bifurcation problem

The finite strain bifurcation approach employed in this paper is heavily influenced by the work of R. Hill on bifurcation at finite strain as represented by the paper [9], and it makes use of developments in [5]. In the current deformed state when the rod/matrix interface has radius R_0, the functional defining the eigenvalue problem for bifurcation is (physical components are used throughout this section)

$$I = \frac{1}{2}\int_V \left(\dot\tau_{ij}\dot\eta_{ij} + \sigma_{ij}\dot u_{k;i}\dot u_{k;i}\right)\, dV \quad (16)$$

Here, in cylindrical coordinates (R, θ, z) identifying material points at bifurcation, $(\dot u_r, \dot u_\theta . \dot u_z)$ are the modal displacement-rate components,

$$\dot u_{r,R} = \partial \dot u_r/\partial R, \quad \dot u_{r,\theta} = R^{=1}(\partial \dot u_r/\partial\theta - \dot u_\theta), \quad \dot u_{r,z} = \partial \dot u_r/\partial z$$

$$\dot u_{\theta,R} = \partial \dot u_\theta/\partial R, \quad \dot u_{\theta,\theta} = R^{=1}(\partial \dot u_\theta/\partial\theta + \dot u_r), \quad \dot u_{\theta,z} = \partial \dot u_\theta/\partial z$$

$$\dot u_{z,R} = \partial \dot u_z/\partial R, \quad \dot u_{z,\theta} = R^{=1}\partial \dot u_z/\partial\theta, \quad \dot u_{z,z} = \partial \dot u_z/\partial z$$

and $\dot\eta_{ij} = (\dot u_{i,j} + \dot u_{j,i})/2$. The non-zero Cauchy (true) stress components in the current state are $(\sigma_r, \sigma_\theta . \sigma_z)$ as given earlier. The symmetric Piola–Kirchhoff stress τ_{ij} is work conjugate to the Lagrangian strain η_{ij} and coincides with the Cauchy stress σ_{ij} at bifurcation for an incompressible material in this reference system. At bifurcation, the principal axes of stress coincide with the cylindrical coordinate system. Increments of τ_{ij} are related to the Jaumann-rate of the Cauchy stress, $\hat\sigma_{ij}$, by

$$\dot\tau_{rr} = \hat\sigma_{rr} - 2\sigma_r\dot\eta_{rr}, \quad \dot\tau_{\theta\theta} = \hat\sigma_{\theta\theta} - 2\sigma_\theta\dot\eta_{\theta\theta}, \quad \dot\tau_{zz} = \hat\sigma_{zz} - 2\sigma_z\dot\eta_{zz}$$

$$\dot\tau_{r\theta} = \hat\sigma_{r\theta} - (\sigma_r + \sigma_\vartheta)\dot\eta_{r\theta}, \quad \dot\tau_{rz} = \hat\sigma_{rz} - (\sigma_r + \sigma_z)\dot\eta_{rz},$$
$$\dot\tau_{\theta z} = \hat\sigma_{\theta z} - (\sigma_\theta + \sigma_z)\dot\eta_{\theta z}$$

For an incompressible neo-Hookean material with ground state shear modulus μ [10,11],

$$\hat\sigma_{rr} = 2\mu{\lambda_r}^2\dot\eta_{rr} - \dot q, \quad \hat\sigma_{\theta\theta} = 2\mu{\lambda_\theta}^2\dot\eta_{\theta\theta} - \dot q, \quad \hat\sigma_{zz} = 2\mu{\lambda_z}^2\dot\eta_{zz} - \dot q$$

$$\hat\sigma_{r\theta} = \mu({\lambda_r}^2 + {\lambda_\theta}^2)\dot\eta_{r\theta}, \quad \hat\sigma_{rz} = \mu({\lambda_r}^2 + {\lambda_z}^2)\dot\eta_{rz},$$
$$\hat\sigma_{\theta z} = \mu({\lambda_\theta}^2 + {\lambda_z}^2)\dot\eta_{\theta z}$$

Combined, the above two sets of equations give the isotropic incremental relation

$$\dot\tau_{ij} = \Lambda\dot\eta_{ij} - \dot q\delta_{ij} \text{ with}$$
$$\Lambda = \frac{2}{3}\mu\left({\lambda_r}^2 + {\lambda_\theta}^2 + {\lambda_z}^2\right) - \frac{2}{3}(\sigma_r + \sigma_\theta + \sigma_z) \quad (17)$$

Equilibrium equations governing bifurcation are obtained from $\delta I = 0$:

$$\frac{\partial(R\dot\tau_{rr})}{\partial R} - \dot\tau_{\theta\theta} + \frac{\partial\dot\tau_{r\theta}}{\partial\theta} + R\frac{\partial\dot\tau_{rz}}{\partial z} + \frac{\partial}{\partial R}\left(R\sigma_r\frac{\partial\dot u_r}{\partial R}\right)$$
$$+\frac{\sigma_\theta}{R}\left(\frac{\partial^2\dot u_r}{\partial^2\theta} - \frac{\partial\dot u_\theta}{\partial\theta}\right) \quad (18)$$
$$-\frac{\sigma_\theta}{R}\left(\frac{\partial\dot u_\theta}{\partial\theta} + \dot u_r\right) + R\sigma_z\frac{\partial^2\dot u_r}{\partial^2 z} = 0$$

$$\frac{\partial \dot{\tau}_{\theta\theta}}{\partial \theta} + \dot{\tau}_{r\theta} + \frac{\partial (R\dot{\tau}_{r\theta})}{\partial R} + R\frac{\partial \dot{\tau}_{\theta z}}{\partial z} + \frac{\partial}{\partial R}\left(R\sigma_r \frac{\partial \dot{u}_\theta}{\partial R}\right) + \frac{\sigma_\theta}{R}\left(\frac{\partial \dot{u}_r}{\partial \theta} - \dot{u}_\theta\right) + \frac{\sigma_\theta}{R}\left(\frac{\partial^2 \dot{u}_\theta}{\partial^2 \theta} + \frac{\partial \dot{u}_r}{\partial \theta}\right) + R\sigma_z \frac{\partial^2 \dot{u}_\theta}{\partial^2 z} = 0 \tag{19}$$

$$R\frac{\partial \dot{\tau}_{zz}}{\partial z} + \frac{\partial (R\dot{\tau}_{rz})}{\partial R} + \frac{\partial \dot{\tau}_{\theta z}}{\partial \theta} + \frac{\partial}{\partial R}\left(R\sigma_r \frac{\partial \dot{u}_z}{\partial R}\right) + \frac{\sigma_\theta}{R}\frac{\partial^2 \dot{u}_z}{\partial^2 \theta} + R\sigma_z \frac{\partial^2 \dot{u}_z}{\partial^2 z} = 0 \tag{20}$$

The conditions across $R = R_0$ require continuity of displacement-rates, $(\dot{u}_r, \dot{u}_\theta . \dot{u}_z)$, and traction-rates, $(\dot{\tau}_{rr} + \sigma_r \partial \dot{u}_r/\partial R,\ \dot{\tau}_{r\theta} + \sigma_r \partial \dot{u}_\theta/\partial R,\ \dot{\tau}_{rz} + \sigma_r \partial \dot{u}_z/\partial R)$.

The field equations for the bifurcation problem comprise the equilibrium equations, (18)–(20), the incremental constitutive relation (17), and the expressions for $\dot{\eta}_{ij}$, together with the continuity conditions across the rod/matrix interface and homogeneous conditions at $R = 0$ and $R \to \infty$ to be discussed shortly. This set is supplemented by the incompressibility equation:

$$\frac{1}{R}\frac{\partial (R\dot{u}_r)}{\partial R} + \frac{1}{R}\frac{\partial \dot{u}_\theta}{\partial \theta} + \frac{\partial \dot{u}_z}{\partial z} = 0 \tag{21}$$

The form for $(\dot{u}_r, \dot{u}_\theta, \dot{u}_z, \dot{q})$ given by (8) provides an exact separation of the field equations leading to a 6th order linear system of odes with $(U(R), V(R), W(R), Q(R))$ as the unknowns for $m = 1$ and a 4th order system (with $V = 0$ and without (19)) when $m = 0$; λ_G is the eigen-parameter for the growth problem and λ_z for the uniform compression problem. Details of this reduction, which is straightforward but lengthy, are omitted. The 6th order system of first order odes can be formed in several ways. An attractive form takes the vector of unknowns as $\mathbf{y} = \left(U, V, W, Q, V', W'\right)$ with a prime denoting the derivative with respect to R. This form is possible because the incompressibility equation, $U' + (U + mV)/R - \beta W = 0$, and its derivative, give U' and U'' in terms of $\mathbf{y}$. The fourth order system deletes V.

The homogeneous conditions at $R = 0$ are $U = W' = 0$ for $m = 0$ and $U + V = 0$, $W = Q = 0$ for $m = 1$. The outer radius of the matrix, R_∞ is taken to be large but finite, and zero displacement rates are imposed. The solution in the matrix decays exponentially with R. If R_∞ is greater than 4 times the axial wavelength, L, to high accuracy the computed results are the same for either zero displacement rates or zero traction rates and, moreover, are insensitive to the choice of R_∞. To evaluate the possibility of bifurcation at any value of λ_G (or of λ_z for the uniform compression), three (two for the 4th order system) linearly independent solutions are constructed each satisfying displacement-rate continuity at the interface. The eigenvalue equation becomes the determinant of a 3×3 (or 2×2) matrix ensuring continuity of the traction-rates.

An extensive study of interface wrinkling and creasing for bonded neo-Hookean material layers is given in [12]. Interface wrinkles and creases are localized at the interface and can have arbitrarily short wavelengths and depths of penetration. A formula for interface wrinkling in [12] accounts for general pre-stretching of one of the layers prior to bonding. This formula can be used to assess the interface in the uniform compression problem and in the limit problem for the fluid pressurized cylindrical cavity, but it is not sufficiently general so that it can be applied to the rod inclusion undergoing constrained growth. Instead, for the growth problem, following an approach analogous to that in [5], we have derived a test for interface wrinkling that is applicable. It accounts for arbitrary stress states on either side of a planar interface (with identical normal components and no shear stress acting on the interface) and it accounts for the current incremental moduli on each side of the interface. This test can be applied to wrinkles oriented in either of the two principal stress directions parallel to the interface. The derivation does not yield a compact formula as in [12], but it reduces to a determinant of a 2×2 matrix that is readily evaluated. This test for wrinkling was employed for assessing the growth problem in the previous section. The results in [12] can be used as a guide as to whether interface creases will occur, which can form before wrinkles. Based on the findings in [12] and our own interface test we are confident that the strains in Fig. 1 fall well below the strains at which interface wrinkling and creasing occur.

5. Closing remarks

The role of the rod inclusion/matrix modulus ratio on the instability mode of growing and compressed rods has been revealed over a wide range of moduli. When the rod has a modulus comparable to the matrix, or less than the matrix, the onset of the instability occurs at relatively large strains and the critical mode can be either axisymmetric or of the bending-type. Neo-Hookean materials have been assumed in this paper and thus in this range quantitative aspects will differ somewhat for other constitutive models. The limit for a soft rod inclusion expanding in a cylindrical matrix cavity is the axisymmetric mode of a fluid pressurized matrix cavity [8], and this limit appears to provide a good approximation even for modestly stiff rods, i.e., $\mu_M/\mu_R \approx 100$. At the other limit of a stiff rod embedded in a compliant matrix, the present results, which are based on an exact 3-D formulation, suggest that the 1-D beam–spring models that have been widely used to predict buckling instabilities provide accurate estimates of the critical stress in the rod and the associated wavelength of the mode for μ_M/μ_R almost as large as 0.1, assuming a good choice of spring model is made.

This paper has limited attention to conditions at bifurcation and no effort has been made to investigate post-bifurcation behavior. The recent study [1] has presented experimental and numerical studies of the post-buckling behavior of compressed stiff elastic rods embedded in elastomeric matrices revealing a rich array of buckling phenomena including modes in which the beam bending deflections become non-planar. The authors of [8] have also presented numerical and experimental results on the post-bifurcation behavior of fluid pressurized cylindrical cavities in elastomers and gels. They find that the initial post-bifurcation behavior is stable under increasing pressure, and the axisymmetric mode develops into a periodic sequence of bulges. The cavitation pressure at which spherical voids expand without limit in a neo-Hookean material is $p_{cavitation}/\mu_M = 5/2$, and this is only modestly above the critical pressure at which bifurcation occurs, $p/\mu_M = 2.054$, suggesting that the bugles may be on the verge of cavitating.

Declaration of competing interest

The authors declare that they have no known competing financial interests or personal relationships that could have appeared to influence the work reported in this paper.

References

[1] T. Su, J. Liu, D. Terwagne, P.M. Reis, K. Bertoldi, Buckling of an elastic rod embedded on an elastomeric matrix: planar vs, non-planar configurations, Soft Matter 10 (2014) 6294–6302.
[2] Y. Zhao, J. Li, Y.P. Cao, X.-Q. Feng, Buckling of an elastic fiber with finite length in a soft matrix, Soft Matter 12 (2016) 2086–2094.
[3] C.P. Brangwynne, F.C. MacKintosh, S. Kumar, N.A. Geisse, J. Talbot, L. Mahadevan, K.K. Parker, D.E. Ingber, D.A. Weitz, Microtubules can bear enhanced compressive loads in living cells because of lateral reinforcement, J. Cell Biol. 173 (2006) 733–741.

[4] A. Goriely, The Mathematics and Mechanics of Biological Growth, Springer, 2017.
[5] R. Hill, J.W. Hutchinson, Bifurcation phenomena in the plane tension test, J. Mech. Phys. Solids 23 (1975) 239–264, footnoteThe second term in the brackets on the right in equation (2.9) in [5] has a sign error. It should be $\mu + (\sigma_1 - \sigma_2)/2$.
[6] Inc., U. Visual Numerics, IMSL Numerical analysis software, 1994.
[7] L.R. Herrmann, W.E. Mason, S.T.K. Chan, Response of reinforcing wires to compressive stress, J. Compos. Mater. 1 (1967) 212–226.
[8] N. Cheewaruangroj, K. Leonavicius, S. Srinivas, J.S. Biggins, Peristaltic elastic instability in an inflated cylindrical channel, PRL 122 (2019) 068003(7).
[9] R. Hill, Bifurcation and Uniqueness in Nonlinear Mechanics of Continua, Muskhelishvili Volume, Soc. Ind. Appl. Math., Philadelphia, Pennsylvania, 1961, pp. 155–164.
[10] M.A. Biot, Chanics of Incremental Deformations, John Wiley & Sons, New York, 1969.
[11] R. Hill, Constitutive inequalities for isotropic elastic solids under strain, Proc. Roy. Doc. Lond. A 314 (1970) 457–472.
[12] L. Jin, D. Chen, R.C. Hayward, Z. Suo, Creases on the interface between two soft materials, Soft Matter 10 (2014) 303–311.